

Received: 2022.05.03

Accepted: 2022.09.09

Available online: 2022.09.15

Published: 2022.10.10

# ***Porphyromonas gingivalis* Activation of Tumor-Associated Macrophages via *DOK3* Promotes Recurrence of Oral Squamous Cell Carcinoma**

Authors' Contribution:  
Study Design A  
Data Collection B  
Statistical Analysis C  
Data Interpretation D  
Manuscript Preparation E  
Literature Search F  
Funds Collection G

ABCDEF 1-3 **Chen-xi Li**  
ABCD 4 **Ying Su**  
ACDG 1-3 **Zhong-cheng Gong**  
ACD 5,6 **Hui Liu**

1 Department of Oral-Maxillofacial Oncology and Surgery, Xinjiang Medical University Affiliated First Hospital, Urumqi, Xinjiang, PR China  
2 School/Hospital of Stomatology, Xinjiang Medical University, Urumqi, Xinjiang, PR China  
3 Stomatological Research Institute of Xinjiang Uygur Autonomous Region, Urumqi, Xinjiang, PR China  
4 College of Software Engineering, Xinjiang University, Urumqi, Xinjiang, PR China  
5 Department of Oral and Maxillofacial Surgery, Shanghai Stomatological Hospital & School of Stomatology, Fudan University, Shanghai, PR China  
6 Shanghai Key Laboratory of Craniomaxillofacial Development and Diseases, Fudan University, Shanghai, PR China

**Corresponding Authors:** Zhong-cheng Gong, e-mail: [gump0904@aliyun.com](mailto:gump0904@aliyun.com), Chen-xi Li, e-mail: [lichenxiuke@gmail.com](mailto:lichenxiuke@gmail.com)  
**Financial support:** This study was funded by the National Natural Science Foundation of China (grant number 82160189), Tianshan Innovation Team of Xinjiang Uygur Autonomous Region (grant number 2021D14001), and Open Project of Shaanxi Clinical Medical Research Center for Dental and Maxillofacial Diseases – School of Stomatology, Xi'an Jiaotong University (grant number 2020YHJB01)  
**Conflict of interest:** None declared

**Background:** Oral squamous cell carcinoma (OSCC) is the most common head and neck malignancy, characterized by high recurrence rate resulting in poor prognosis. *Porphyromonas gingivalis*, most closely correlated with chronic periodontitis, is increasingly thought to play a significant role in OSCC development via influencing tumor-associated macrophages. However, its specific function remains unclear. In this study, we attempted to explore the mechanism of action of *P. gingivalis* in the recurrence of OSCC by bioinformatics analysis, to lay a foundation for subsequent basic experiments.

**Material/Methods:** The *P. gingivalis*-infected macrophage microarray dataset (GSE24897) and the OSCC advanced relapse patient microarray dataset (GSE87593) were retrieved from the Gene Expression Omnibus (GEO) database. Differentially-expressed genes (DEGs) were screened using R system, and the intersected DEGs were analyzed for functional enrichment, and protein-protein interaction (PPI) networks were constructed. The expression of significant DEG in GSE24897 microarray was assessed to determine its effect on macrophage immune infiltration in pancreatic cancer by applying the TIMER 2.0 repository. To detect the expression of *DOK3* in OSCC specimens, immunohistochemical (IHC) assay was used.

**Results:** A total of 106 co-expressed DEGs were upregulated and 131 were downregulation. The biological processes were mainly enriched in DNA-templated transcription terms, the cellular component enrichment was mainly enriched in the nucleus terms, and the molecular function enrichment was mainly enriched in protein-binding function terms. Kyoto Encyclopedia of Genes and Genomes (KEGG) analysis found that the DEGs were mainly enriched in the MAPK signaling pathway. Overall analysis of the PPI network showed a significant aggregation, with the top 10 hub co-expressed genes (*CASP3*, *FYN*, *HNRNPA2B1*, *NR3C1*, *RELA*, *REL*, *POLR2F*, *RAN*, *RHOA*, and *STAT5B*). *DOK3* is significantly upregulated in *P. gingivalis*-infected macrophages, which is associated with macrophage infiltration and differentiation. There was more positive *DOK3* staining in the group with *P. gingivalis* infection.

**Conclusions:** *P. gingivalis* can affect the recurrence of OSCC by increasing the expression of *DOK3* in TAMs, which may be involved in activation of signaling pathways such as TNF and MAPK.

**Keywords:** ***DOK3* Protein, Human • Macrophage Activation • Neoplasm Recurrence, Local • *Porphyromonas gingivalis* • Squamous Cell Carcinoma of Head and Neck • Tumor Microenvironment**

Full-text PDF: <https://www.medscimonit.com/abstract/index/idArt/937126>



3320 1 8 68

## Background

Cancer of the oral cavity has a high recurrence and high staging at diagnosis, which often does not allow surgical treatment because the interventions are too destructive and have secondary complications; therefore, the treatment of choice is chemoradiotherapy [1]. Oral squamous cell carcinoma (OSCC) is the most common subgroup of head and neck malignancies, which can develop in all parts of the oral cavity, resulting directly from apparently normal mucosa or progressively from potentially malign disorders [2]. Annually, there are around 400 000 new cases diagnosed all across the globe, accounting for 2% of all cancers [3]. Patients with advanced OSCC have poor prognosis due to strong invasive ability, high recurrence rate, and lymph node metastasis [4]. Locoregional recurrence is frequent (approximately 32.7–44.9%) [5–7] and remains a critical issue in clinical management of advanced-stage OSCC [8].

Increased attention has focused on the interaction between oral microbiome and OSCC in the past few decades [9]. The accumulated evidence indicates that chronic periodontitis is one of the pathogenic factors resulting in OSCC [10–13], which was found to increase the incidence of OSCC by 5.23-fold [14]. Microbiota homeostasis plays important roles in health and disease. Dysbiosis of oral flora can disrupt the host immune defense, thus deeply affecting tumorigenesis [15,16]. *Porphyromonas gingivalis* is a gram-negative absolute anaerobic bacterium that is a crucial bacterial pathogen of OSCC characterized by invading the cellular circle and normal physiological metabolism of epithelial cells, interfering with the host immune system, and producing a toxic effect of inhibiting programmed cell death [17,18]. Many anatomical structures (eg, gingiva, buccal mucosa, dorsum of the tongue, lingual margin, hard and soft palate) are easily colonized by various types of microflora [19,20]; therefore, *P. gingivalis* can prolong the time of contact with tumor cells to promote OSCC progression [9]. Tuominen et al [21] has reported that *P. gingivalis* can inhibit apoptosis, activate cell proliferation, promote cell invasion, induce chronic inflammation, and directly produce carcinogens. *P. gingivalis* has been detected in abundance in the oral cavity of patients with OSCC [22], suggesting it is an independent bacterial factor that raises the risk of death in OSCC patients [23]. Abnormal aggregation of *P. gingivalis* can cause local microecological imbalance of the oral cavity and is a dominant species in periodontitis, and further impact is the formation of a tumor microenvironment (TME) that is closely associated with oro-digestive carcinogenesis [24]. TME refers to a restricted internal environment constituted by locally tumor-associated infiltrating mesenchymal cells (eg, macrophages, fibroblasts, neutrophils, epithelial/endothelial cells) and their secretory extracellular matrix (ECM) together with inner cancer cells [25,26].

Tumor-associated macrophages indeed are among the most plentiful and important tumor-infiltrating immune cell types in TME. They have great plasticity in function, which can present diverse phenotypes to act within distinct microenvironments based on their biogenesis and biological properties [27]. According to different regulatory signals and states, macrophages can be categorized into 2 polarizations: classical activation type (M1 type) and alternative activation type (M2 type) [28]. More importantly, the pro-tumor effects of TAMs have strong links with their M2 polarized phenotype [29,30]. The downstream of kinase (*DOK*) is a new type of family of tyrosine residue phosphorylated proteins that participates in the regulation of tumor cell growth [31]. To date, there are 7 known human *DOK* genes (*DOK1* to *DOK7*) that participate in regulation of various signaling pathways, such as cell growth, proliferation, migration, and apoptosis [32,33]. As one of these subtypes, the *DOK3* gene, located at 5q35.3, exon 8 [34], is an immune-specific possessing specific pattern of expression in immune cells [36,36]. Macrophages studies showed it can downregulate the macrophage response stimulated by granulocyte macrophage colony-stimulating factor (GM-CSF) [37], and can be strongly positively associated with marker genes in M2 TAMs [35].

Herein, we hypothesized that *P. gingivalis* might affect the macrophages infiltrated in TME to give rise to OSCC recurrence through modulation of *DOK3*, so the possible molecular mechanism was explored by performing bioinformatics analysis to provide research directions for future experimental studies.

## Material and Methods

### Ethics

Our study was reviewed and approved by the Ethics Committee at the First Affiliated Hospital of Xinjiang Medical University, Urumqi, PR China (approval number: K202107-06). Procedures in this research were completed in keeping with the standards of the Helsinki Declaration and laboratory guidelines of research in China. Written informed consent was not applicable.

### Data Preparation

To screen the datasets related to *P. gingivalis* infection of macrophages, as well as late recurrence of OSCCs, we downloaded 2 expression profile sequencing datasets (GSE24897 and GSE87593, respectively) from the Gene Expression Omnibus (GEO) (<http://www.ncbi.nlm.nih.gov/geo>) database using GSE24897 by GPL570 Platform (Affymetrix Human Genome U133 Plus 2.0 Array) and GSE87593 by GPL14550 Platform (Agilent-028004 SurePrint G3 Human GE 8x60K Microarray). Their probes were converted to the corresponding gene symbols

based on annotation information on the platform. GSE24897 dataset contains 3 sets of uninfected macrophages and 3 sets of *P. gingivalis*-infected macrophage samples, and the GSE87593 dataset contains 8 sets of OSCC late non-recurrent tissue samples and 8 sets of OSCC late recurrent tissue samples.

### Differentially-Expressed Gene Analysis

The 2 datasets were separately analyzed using the Limma package in R software version 4.0.2 (R Foundation for Statistical Computing, Vienna, Austria). The probes without corresponding gene symbols or with multiple gene symbols were removed or taken as intersection. The differentially-expressed genes (DEGs) were screened and heat-mapped using the R heatmap package. Accordingly, differences were considered statistically significant with logFC (fold change) >1 and adj. *P* value <0.01.

### Functional Annotations Analysis

We employed DAVID (Database for Annotation, Visualization and Integrated Discovery) (<https://david.ncifcrf.gov/>) resources to obtain information for gene ontology (GO), including biological processes, cellular component, and molecular function. The Kyoto Encyclopedia of Genes and Genomes (KEGG) pathway analysis was used to annotate the potential functions. A significance level of *P*<0.05 was set as the cutoff criteria and the plots were constructed by the gplots package in R software.

### Protein-Protein Interaction Analysis

The DEGs were enrolled in a protein-protein interaction (PPI) network through the STRING database (<https://string-db.org/>). The filtering condition was medium confidence (0.400), and isolated nodes were excluded to generate the PPI network. The hub genes were calculated using Hubba plug-in of Cytoscape software version 3.8.0 (Free Software, Boston, MA, USA).

### Macrophage Infiltration

We used the TIMER 2.0 online tool (<http://timer.comp-genomics.org/> or <http://timer.cistrome.org/>) to explore macrophage infiltrates across diverse cancers using the immune module.

### Collection of Clinical Samples

Fifty patients with recurrent OSCC admitted to our center from January 2020 to June 2022 were selected for the study, of whom 27 were males and 23 were females, aged 55~75 years. All patients were tested for *P. gingivalis* before enrollment (the detection method for *P. gingivalis* is shown in **Supplementary Figure 1**), of which 25 were *P. gingivalis*-positive and 25 were *P. gingivalis*-negative. All patients in this study voluntarily participated and signed the informed consent form. There was

no significant difference between the 2 groups in terms of general information such as sex and age (*P*>0.05). The use of human samples in this study was approved by our center's Ethics Committee and was performed according to the STROBE (Strengthening the Reporting of Observational Studies in Epidemiology) statement.

### Histopathological Evaluation

Fresh OSCC tissues excised during clinical procedures were placed in 4% formaldehyde solution for fixation, and then were dehydrated, paraffin-embedded, and serially sectioned to 4- $\mu$ m thickness. The sections were dewaxed in xylene; hydrated in ethanol with gradients of 100%, 95%, 90%, and 85% for 5 min each. Antigen repair was performed with 10 mmol/L sodium citrate buffer for 15 min, washed 3 times with PBS after natural cooling, and reacted with peroxidase blocker for 15 min to block endogenous peroxidase, then washed 3 times with PBS and incubated with goat serum. Sections were incubated with DOK3 monoclonal antibody (Abcam, ab236609, 1: 500) and incubated overnight at 4°C in a refrigerator. After rewarming for 2~5 min, goat anti-rabbit IgG was added after washing with PBS and incubated at room temperature for 25 min, then washed 3 times with PBS, and horseradish peroxidase-labeled streptavidin working solution was added for 15 min. After washing 3 times with PBS, the DAB kit (Beyotime, Shanghai, China) was used for 3~5 min; hematoxylin was used for restaining, 1% hydrochloric acid alcohol fractionation for 1~2 s, and water was used to return the blue. After natural drying, 10% neutral gum was used to seal the film. Double-blind scoring was performed by 2 professional pathologists. Eight fields of view per section were randomly selected for observation at 200 $\times$  and 400 $\times$ .

### Statistical Analysis

All data-mining work was performed using the packages Limma (Version 3.46.0) [38], MethylMix (Version 2.20.0) [39], clusterProfiler (Version 4.3.1) [40], survminer (Version 0.4.9), survival (Version 3.2.13), glmnet (Version 4.1.2) [41], pheatmap (Version 1.0.12), corrplot (Version 0.90), timeROC (Version 0.4) [42], WGCNA (Version 1.70.3) [43], maftools (Version 2.6.5) [44], and pRRophetic (Version 0.5) implemented in R software, version 4.0.2 (R Foundation for Statistical Computing, Vienna, Austria). When measurement data were normally distributed, data were expressed by mean $\pm$ standard deviation (SD), and an independent samples *t* test was used for comparison of 2 groups, while the chi-square test was used for comparison of count data. For all analyses, two-tailed *P*<0.05 was set as the threshold for determining statistical significance. Differences were considered significant if \* *P*<0.05; \*\* *P*<0.01; \*\*\* *P*<0.001, \*\*\*\* *P*<0.0001.

**Results**

**Identification of DEGs**

After normalizing the expression profile of sequencing data,

the distributions of differential gene expression between 2 samples were visualized using volcano plots (Figure 1A, 1B). A total of 747 differentially-expressed genes were identified in the GSE24897 dataset, including 496 upregulated genes and 251 downregulated genes (Figure 1C), while 747

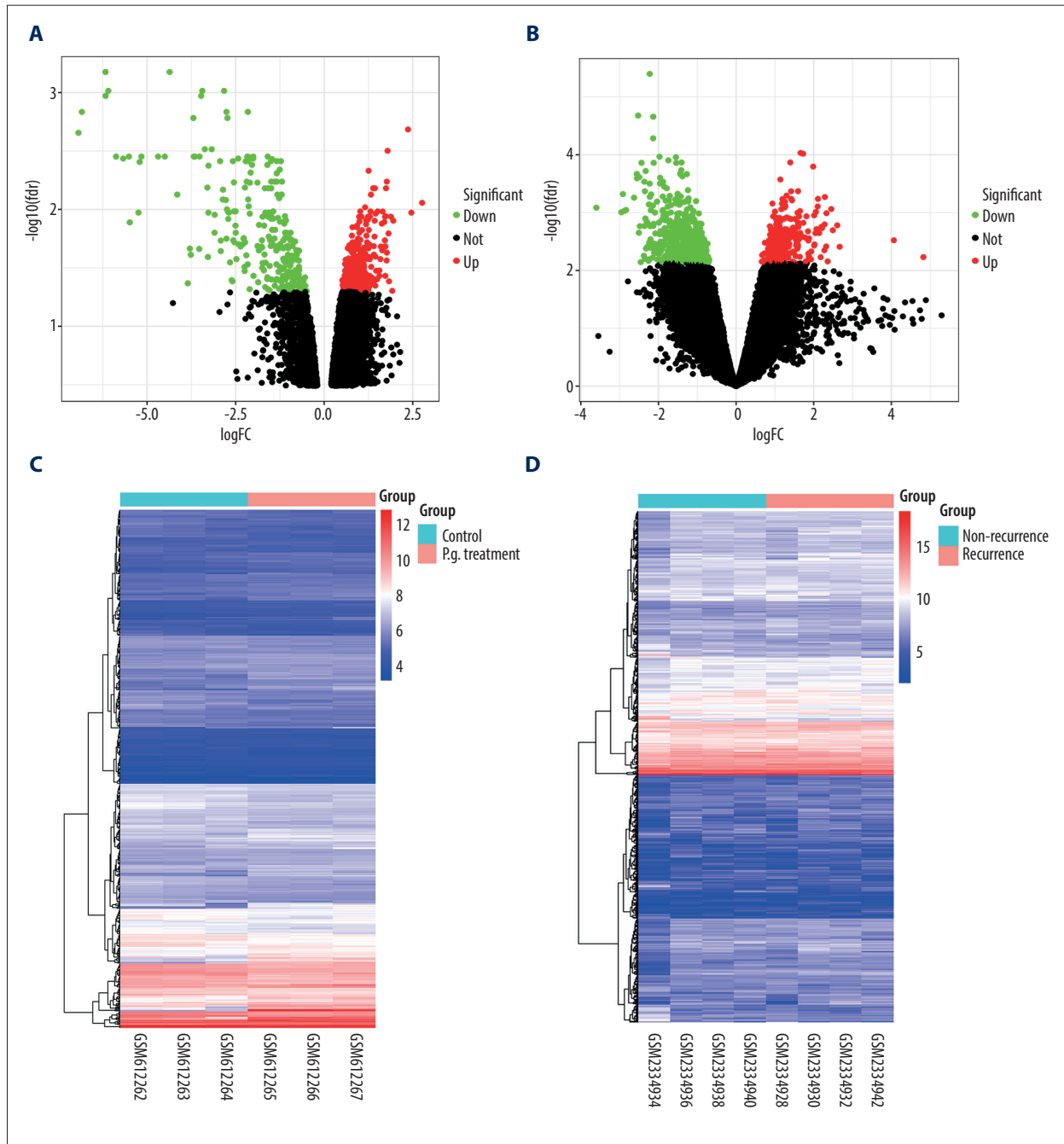


**Figure 1. Distributions of differentially-expressed genes.** (A, B) The volcano plot of GSE24897 and GSE85793. Green dots represent significantly downregulated genes, red dots represent significantly upregulated genes, and black dots represent insignificantly changed genes. (C, D) The heatmaps of DEGs. Blue color represents low expression genes, red color represents high expression genes, and different color brightness represents gene expression. R software 4.1.3 version was used for visualization.

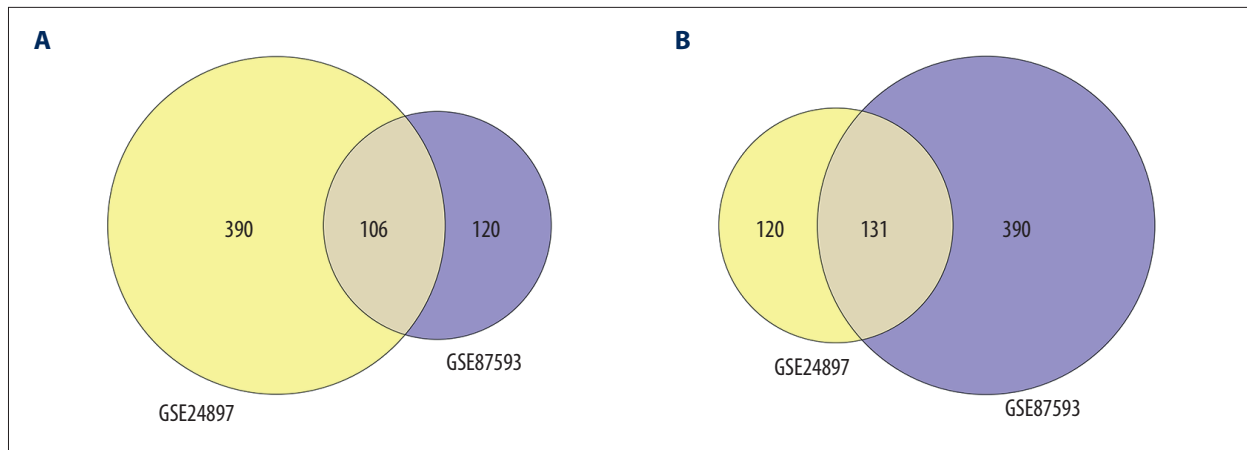


**Figure 2. Venn plots of differentially-expressed genes (DEGs).** Venn plots of DEGs showing upregulated (A) and downregulated genes (B). R software 4.1.3 version was used for visualization.

**Table 1.** The GO and KEGG enrich terms.

Term	Fold enrichment	p-Value	Count
<b>BP enrichment</b>			
Transcription, DNA-templated	1.68	0.00	40
Negative regulation of granulocyte differentiation	30.72	0.00	3
Protein targeting to vacuole	30.72	0.00	3
Golgi to plasma membrane protein transport	12.14	0.00	4
Positive regulation of neuron projection development	5.52	0.00	6
Somatic stem cell population maintenance	6.30	0.01	5
Blood vessel development	8.62	0.01	4
Positive regulation of I-kappaB kinase/NF-kappaB signaling	3.56	0.01	7
Lymph node development	14.46	0.02	3
activation of MAPKK activity	7.12	0.02	4
Positive regulation of type I interferon production	6.42	0.02	4
Development of secondary female sexual characteristics	81.91	0.02	2
Viral process	2.47	0.03	9
Positive regulation of erythrocyte differentiation	10.24	0.03	3
Response to tumor necrosis factor	9.83	0.04	3
Peptidyl-tyrosine phosphorylation	3.21	0.04	6
Endodermal cell differentiation	9.10	0.04	3
Glutamate secretion	8.78	0.05	3
Hematopoietic progenitor cell differentiation	4.96	0.05	4
Creatinine metabolic process	40.96	0.05	2
Positive regulation of viral transcription	8.47	0.05	3
Transcription from RNA polymerase II promoter	1.92	0.05	12

**Table 1 continued.** The GO and KEGG enrich terms.

Term	Fold enrichment	p-Value	Count
<b>CC enrichment</b>			
Nucleus	1.45	0.00	92
Cytoplasm	1.38	0.00	84
Cytosol	1.52	0.00	59
Nucleoplasm	1.57	0.00	51
Microtubule organizing center	3.91	0.01	7
Neuron projection terminus	19.74	0.01	3
Apical part of cell	5.70	0.01	5
Centrosome	2.41	0.01	12
Spindle	4.24	0.01	6
Trans-Golgi network membrane	5.15	0.02	5
Midbody	3.98	0.02	6
Trans-Golgi network	3.77	0.02	6
Microtubule	2.48	0.03	9
Membrane raft	2.91	0.03	7
TAP complex	57.04	0.03	2
Recycling endosome	3.89	0.04	5
Lysosomal membrane	2.50	0.04	8
<b>MF enrichment</b>			
Protein binding	1.24	0.00	127
Receptor signaling protein serine/threonine kinase activity	9.70	0.00	6
Transcriptional activator activity, RNA polymerase II distal enhancer sequence-specific binding	13.71	0.00	4
RNA polymerase II distal enhancer sequence-specific DNA binding	6.59	0.01	5
Metal ion binding	1.53	0.01	37
Poly(A) RNA binding	1.67	0.02	22
Activin-activated receptor activity	85.69	0.02	2
Transferase activity	4.46	0.03	5
Peptide antigen-transporting ATPase activity	57.13	0.03	2
TAP1 binding	42.85	0.05	2
<b>KEGG enrichment</b>			
Tuberculosis	3.49	0.01	8
TNF signaling pathway	4.33	0.01	6
Focal adhesion	3.00	0.02	8
Neurotrophin signaling pathway	3.86	0.02	6

**Table 1 continued.** The GO and KEGG enrich terms.

Term	Fold enrichment	p-Value	Count
<b>KEGG enrichment</b>			
Viral myocarditis	5.42	0.04	4
MAPK signaling pathway	2.44	0.04	8
Apoptosis	4.99	0.04	4
Viral carcinogenesis	2.64	0.05	7

differentially-expressed genes were identified in the GSE87593 dataset, including 226 upregulated genes and 521 downregulated genes (Figure 1D). Posterior to taking the intersection of the 2 collections, there were 106 genes in common among all upregulated genes (Figure 2A) and 131 genes in common among all downregulated genes (Figure 2B).

### Functional Analysis of DEGs

To understand the biological meaning behind lists of DEGs, enrichment analysis of signaling pathways and functions was performed using DAVID (Table 1). Biological processes (BP) were mainly enriched in DNA-templated transcription terms (Figure 3A), the cellular component (CC) enrichment was mainly enriched in the nucleus terms (Figure 3B), and molecular function (MF) enrichment was mainly enriched in protein-binding function terms (Figure 3C). KEGG enrichment analysis found that the genes were predominantly enriched in the MAPK signaling pathway (Figure 3D).

### The PPI Network of the Co-Expression of DEGs

The co-expression of DEGs was imported into the online STRING Data Resources to derive the PPI network, which showed a total of 225 nodes and 232 edges. After hiding the isolated nodes in the network, 198 expected nodes remained, with a PPI enrichment *P* value of 0.0108. The overall analysis of the network showed a significant aggregation (Figure 4). Using cyto-Hubba software package, all the proteins in PPI network were calculated by applying maximum correntropy criterion (MCC) algorithm, which displaying that the top 10 ranked genes were *CASP3*, *FYN*, *HNRNPA2B1*, *NR3C1*, *RELA*, *REL*, *POLR2F*, *RAN*, *RHOA*, and *STAT5B* (Figure 5).

### The Relationship Between *DOK3* Expression and Macrophage Infiltration

To investigate the effect of *DOK3* expression on macrophage infiltration, we first analyzed the expression of *DOK3* in *P. gingivalis* infection of macrophages microarray. The analysis revealed that the expression of *DOK3* significantly increased

after macrophages were treated with *P. gingivalis* (Figure 6A,  $P < 0.0001$ ). The effect of *DOK3* on macrophage infiltration was further analyzed, showing that expression of *DOK3* affected the infiltration of M1 and M2 TAMs in oral cancer (Figure 6B,  $P < 0.05$ ).

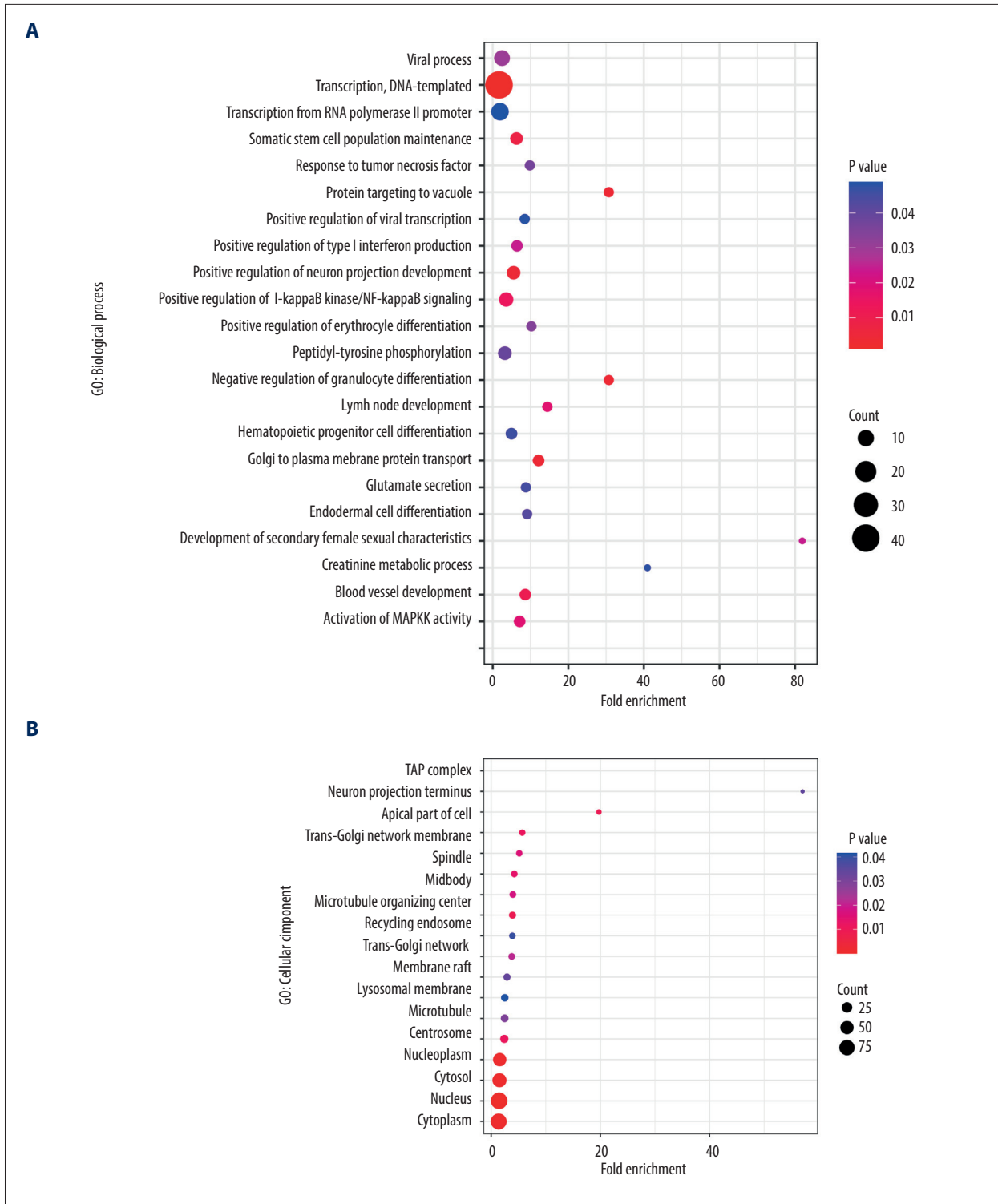
### Expression of *DOK3* in Patients with Recurrent OSCC with Different *P. gingivalis* Infections

To confirm the expression of *DOK3* in patients with different *P. gingivalis* infections, we collected oral cancerous tissues from patients with recurrent OSCC through clinical biopsy and divided the patients into *P. gingivalis*-infected and non-infected groups by *P. gingivalis* detection. The expression of *DOK3* in 2 groups was detected by immunohistochemistry (ICH), and the results showed that the *DOK3* staining was stronger in the group with *P. gingivalis* infection than in the group without *P. gingivalis* infection (Figure 7).

### Discussion

Progress in surgical skills of radical reconstruction, radiotherapeutics, chemotherapy approaches, anti-cancer-immune-drug development, and molecular characterization of OSCC in this new millennium were expected to lead to better prognoses for OSCC patients. However, clinical outcomes have barely improved in recent years, particularly for OSCC, and the short-term and long-term treatment-associated relapse rates are still high. Tobacco and alcohol consumption, as well as the microbiological agents mentioned in the Introduction section above, have important roles in the occurrence and progression of OSCC [45,46]. One of the reasons why high morbidities of recurrence and metastasis are observed among OSCC cases is the rich blood supply and lymphatic reflux of this anatomical site [47]. Another reason may be the easy bacterial colonization under suitable conditions, supported by the connection between the respiratory and digestive tracts [48].

Different severity of factors, including microbial dysbiosis and immune dysfunction, likely contribute to oral tumorigenesis.





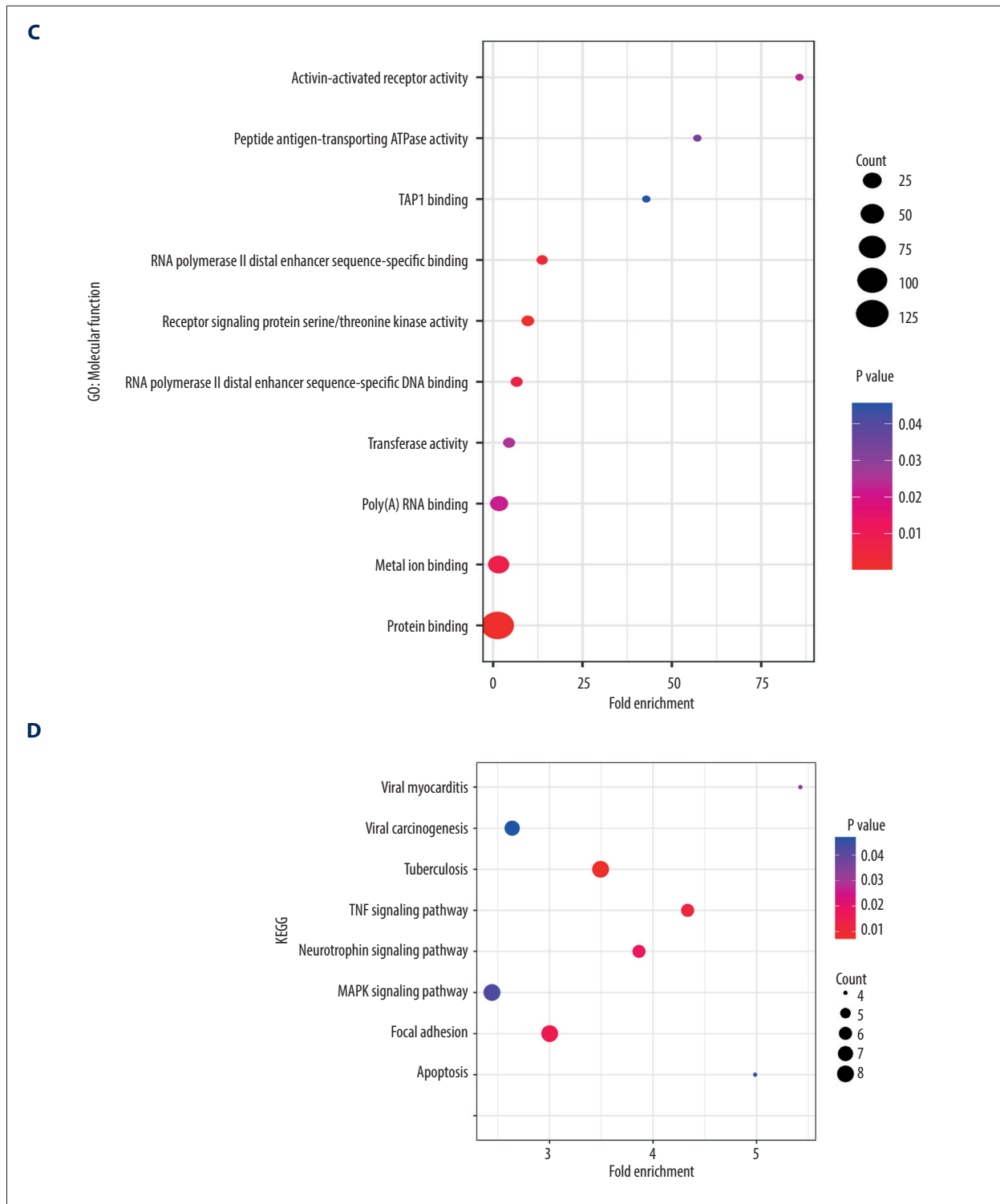


**Figure 3. The GO and KEGG analysis.** The significant enrichment terms in (A) BP, (B) CC, and (C) MF were shown using a scatter plot. The significant pathways involved in (D) KEGG enrichment was shown using a scatter plot. Colors represent the P values and sizes of the spots represent the counts of genes. R software 4.1.3 version was used for visualization.

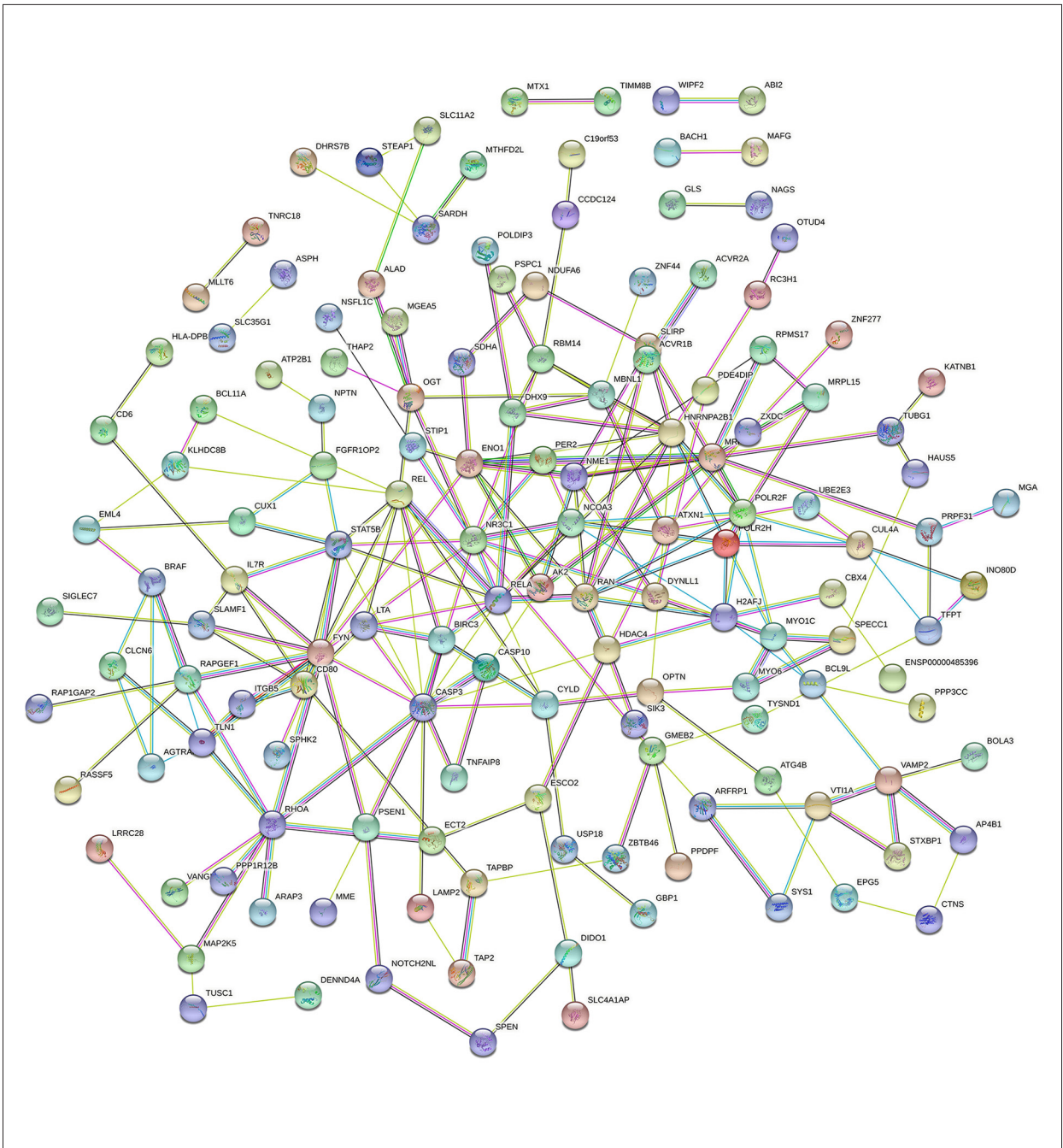


**Figure 4. The PPI network.** A network of protein–protein interactions (PPI) was built using STRING. Different nodes represent different proteins and the edges represent the degree of connection between proteins. String version 11.5 was used for visualization.

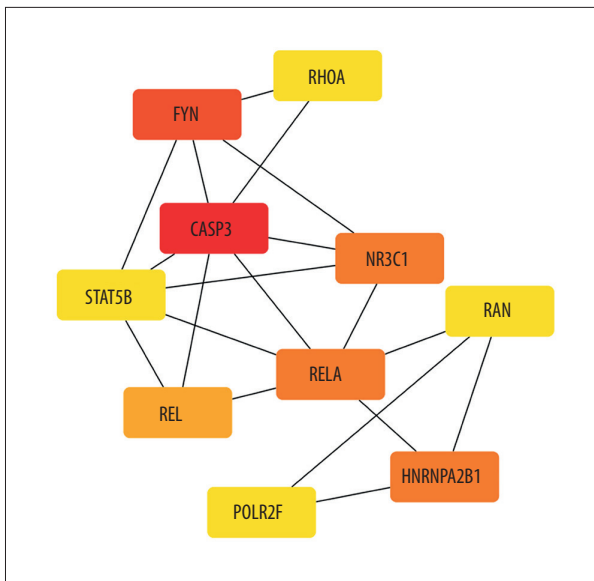


**Figure 5. Hub genes computed by MCC algorithm.** The top 10 hub genes were obtained by the MCC algorithm. Cytoscape version 3.9.0 was used for visualization.

Many studies have confirmed that microorganisms directly affect the activities of primary epithelial and OSCC cells, which mediates assorted biological behaviors in a process that starts from benign lesions, progresses to intermediate proliferative stages, and eventually deteriorates into oral cancer in situ or generating sharp invasion, proving its synergism in cancerous growth [23,49]. This suggests that the elements and/or transformation of microbial communities can have a great impact on oral carcinogenesis [50]. Foremost among these is *P. gingivalis*, which promotes OSCC progression via generating a cancer-promoting microenvironment composed of bacterial production, tumor cells, and infiltrating immune cells [51]. In the field of high-throughput gene sequencing, *P. gingivalis* outer membrane vesicles containing different packaged small RNAs is a novel insight into the host-pathogen interaction, whereby *P. gingivalis* boosts the invasion and migration of OSCC in vitro [52]. *P. gingivalis*-induced inflammatory efficacy is the causative keystone sustaining and stimulating a pre-cancerous niche [53] to continuously generate reactive oxygen species, reactive nitrogen intermediates, inflammatory chemokines, and pyroptosis-related cytokines that exacerbate the accumulation of mutations by triggering DNA damage, reducing genetic stability, and causing epigenetic alterations, which subsequently promote cellular carcinogenesis [54-56].

Oral epithelial cells infected by *P. gingivalis* enhance the proliferation of pre-cancerous cells, as well as the angiogenesis, local invasion, and distal metastasis of cancer cells, and, critically, the formation of chronic inflammation into the TME [47,57,58]. Entry of microbial metabolites into the TME promotes tumor progression by eliciting tumor-potentiating

immune cell responses [51]. Part of our preceding work found that CXCL2 and neutrophils were markedly increased in OSCC tissues and the TME infected by *P. gingivalis*, indicating that *P. gingivalis* and CXCL2 are involved in the recruitment of neutrophils, which contributes to the progression of OSCC [59]. A recent study also reported that *P. gingivalis* can accelerate inflammation-and-tumor formation by interfering with the migration of macrophages and inhibiting their phagocytosis of apoptotic neutrophils [60]. TAMs represent yet another considerable cell subpopulation that accounts for more than half of the immune microenvironment of OSCC [61]. In this present study, we obtained 2 sequencing datasets: (1) microarray of macrophages treated with *P. gingivalis*, and (2) microarray of OSCC advanced relapse. According to bioinformatics analysis, a total of 237 co-expressed DEGs were identified between the 2 datasets, including 106 upregulated genes and 131 down-regulated genes. We performed functional de novo analysis using GO and KEGG to determine which enriched points of entry are associated with the TME. In BP enrichment, we found positive regulation of I- $\kappa$ B kinase/NF- $\kappa$ B signaling, activation of MAPK activity, response to tumor necrosis factor, the endodermal cell differentiation, glutamate secretion viral process, and positive regulation of viral transcription. In KEGG analysis, we also observed significant enrichment of co-expressed genes in the TNF signaling pathway, MAPK signaling pathway, apoptosis, and viral carcinogenesis. A definite correlation between the presence of *P. gingivalis* and Epstein-Barr virus (EBV) infection has been established, as well as the mechanisms by which EBV and *P. gingivalis* independently or synergistically can collaborate, indicating the oral cavity is the principal site where both of them are harbored due to their oncogenic potential [62]. Collectively, the results of our enrichment analysis showed that the changes in cell-biology-related functions and pathways caused by *P. gingivalis* may be consistent with those caused by viral infections. The enrichment of the aforementioned points of entry analyzed in our study suggests that the occurrence of *P. gingivalis* infection in macrophages can give rise to alterations in cellular biological functions and pathways, which in turn lead to alterations in the TME and promote tumorigenesis. To further screen the hub genes of co-expressed DEGs, we established a PPI network and further calculated the network by MCC algorithm to find the 10 most expressed genes: *CASP3*, *FYN*, *HNRNPA2B1*, *NR3C1*, *RELA*, *REL*, *POLR2F*, *RAN*, *RHOA*, and *STAT5B*. Previous studies have found that *CASP3* and *STAT5B* are involved in formation of the TME and are associated with tumorigenesis in some solid neoplasms; genetic defects including mutations in *RHOA* and *FYN* have been examined to reveal inactivate immunosurveillance in angioimmunoblastic T cell lymphoma [63-65].

Significantly higher expression level of *DOK3* was associated with the TME of OSCC infected via *P. gingivalis*. We found that the *DOK3* staining was stronger in the group with *P. gingivalis*

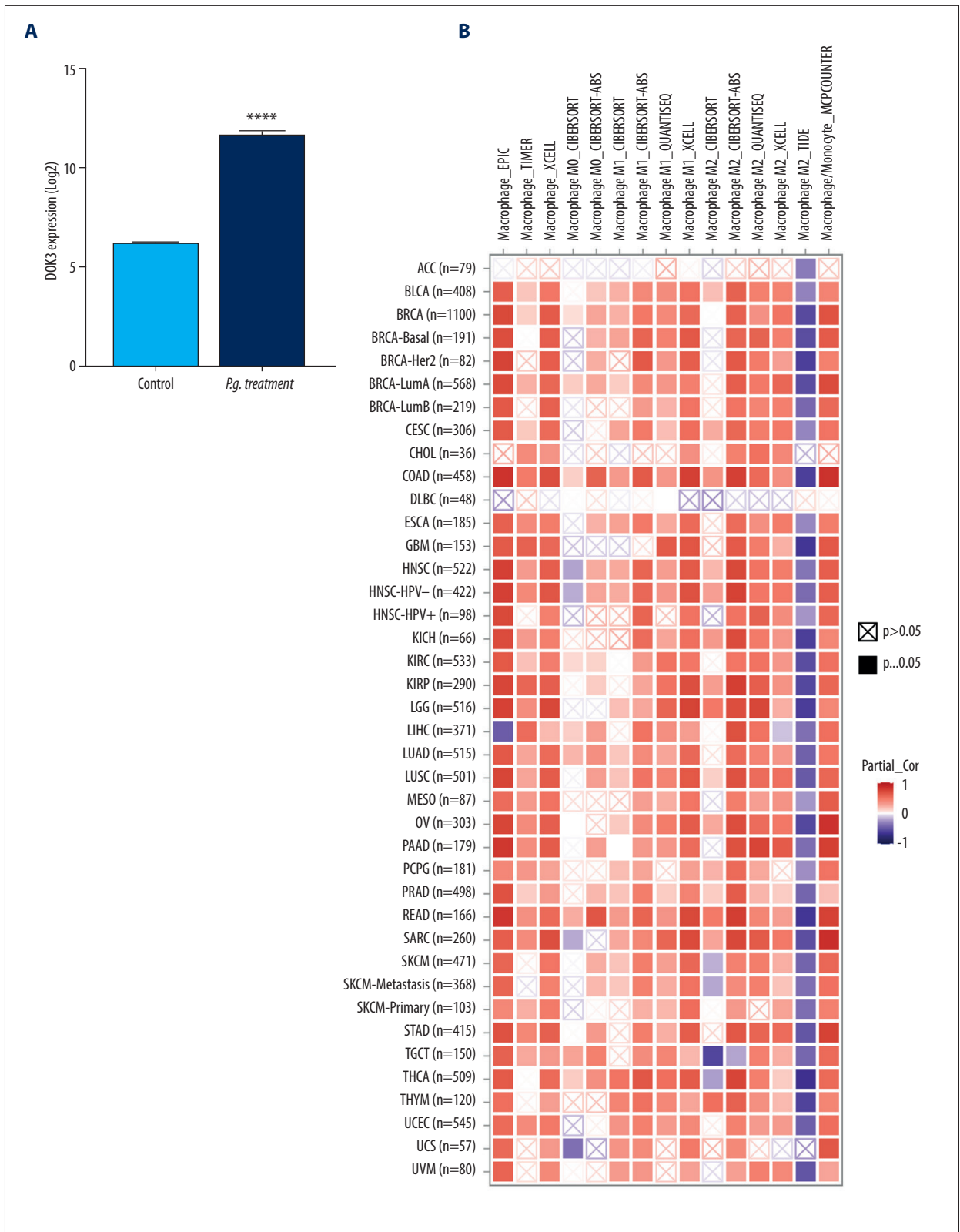


**Figure 6.** The relationship between *DOK3* expression and macrophage infiltration. **(A)** The *DOK3* expression in *P. gingivalis* infection of macrophages microarray; **(B)** macrophages infiltration affected by *DOK3*. GraphPad Prism 8 was used for visualization in Figure 5A, and the TIMER 2.0 online tool was used for visualization in Figure 5B.

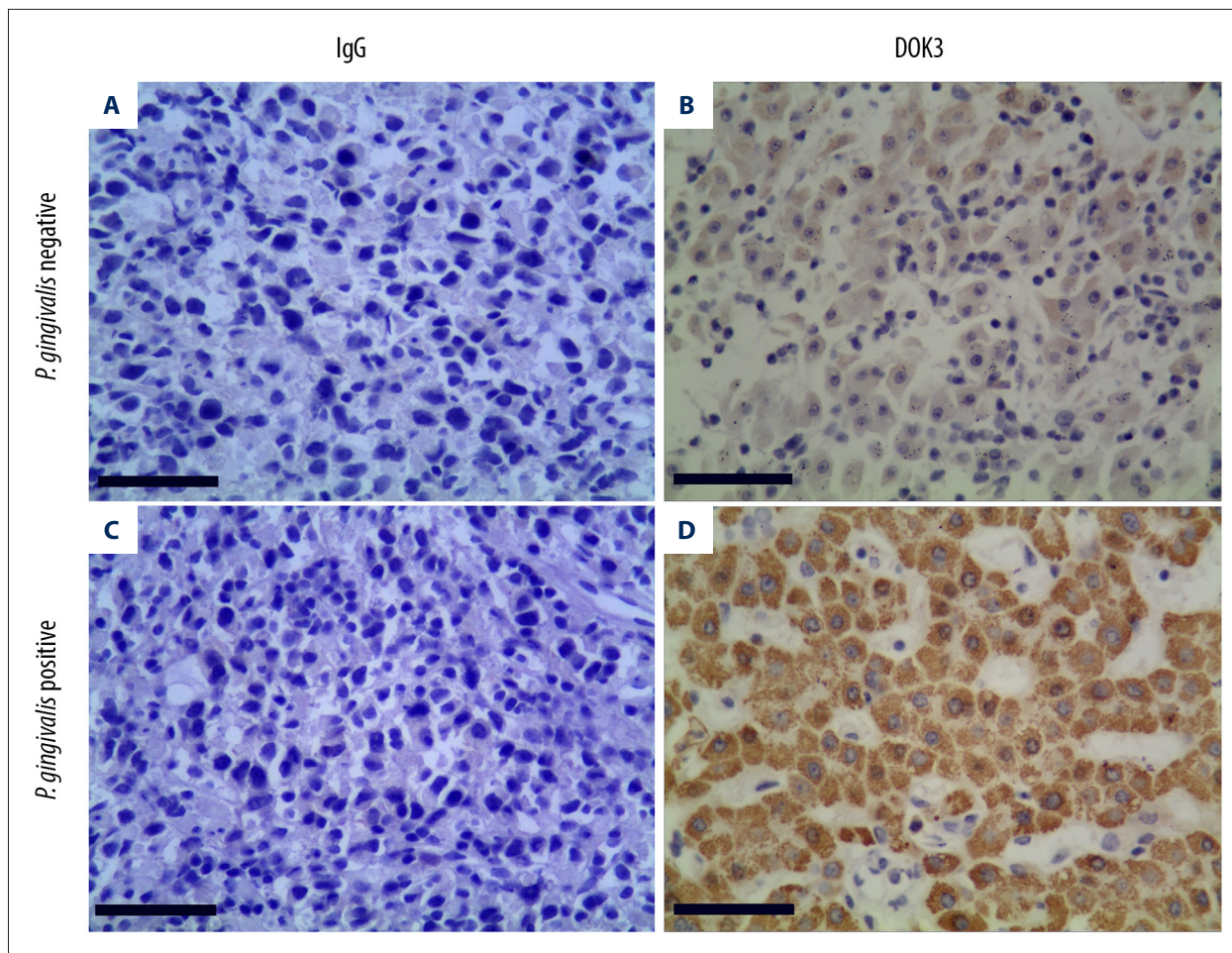


**Figure 7.** The expression of *DOK3* in recurrent OSCC patients with different *P. gingivalis* infections (**B and D**, 200×) compared with non-immune IgG staining as a control (**A and C**, 200×). The yellow-stained granules represent *DOK3* staining-positive cells, and the larger yellow staining area represents higher *DOK3* expression.

infection. In another tumor study, *DOK3* was reported to affect colorectal cancer tumorigenesis [66]. *DOK3* can function as an adapter molecule in the negative regulation of immunoreceptor signaling in macrophages, and influences immune microenvironment to result in an aggressive growth pattern of cancer cells manipulated by a high degree of local macrophage infiltrations. For the analyses of macrophage infiltration of distinct cancers, we ascertained that *DOK3* is obviously highly expressed in macrophages of *P. gingivalis*, affirming that *DOK3* is a vital regulator of innate immune responses in macrophages [67]. *DOK3* was also found to be strongly positively correlated with marker genes of TAMs and M2 macrophages, but not M1 [35], and the ability M2 macrophages relies heavily on the elevation of *DOK3* expression in a glioma study repertoire, which led to poor prognosis [68]. Our analysis of the TIMER2.0 database also showed that *DOK3* expression is associated with M2 polarization differentiated from TAMs.

### Limitations

The present study is a bioinformatics analysis based on data provided by a public database (GEO), and although we found high expression of *DOK3* in tumor tissues of patients with recurrent OSCC and *P. gingivalis* infection by ICH detection using clinical specimens, the generalizability of our final conclusions remains limited. In the future, we will confirm through experimental in vitro cellular studies and in vivo animal studies that *P. gingivalis* affects TAMs infiltration and promotes tumor malignant progression in recurrent OSCC TME by *DOK3* regulation.

### Conclusions

Our study shows the participation of *Porphyromonas gingivalis* in the TME, as well as how *P. gingivalis* possibly modulates TAMs in OSCC. Via the role of *DOK3* in TAMs, high expression of *DOK3* is regulated in TNF/MAPK signaling pathways. The

contribution of the TME has been important in identifying the role of components other than tumor cells that cause the development of oral cancer, thus changing the outlook. As the key molecule, *DOK3* might be the keystone modulator of M2 macrophage polarized from infiltrated TAMs, in order to further mediate immune surveillance/escape to promote cancerous progression.

**Data Availability Statement**

The raw data supporting the conclusions of this article will be made available by the authors upon reasonable request.

**Acknowledgements**

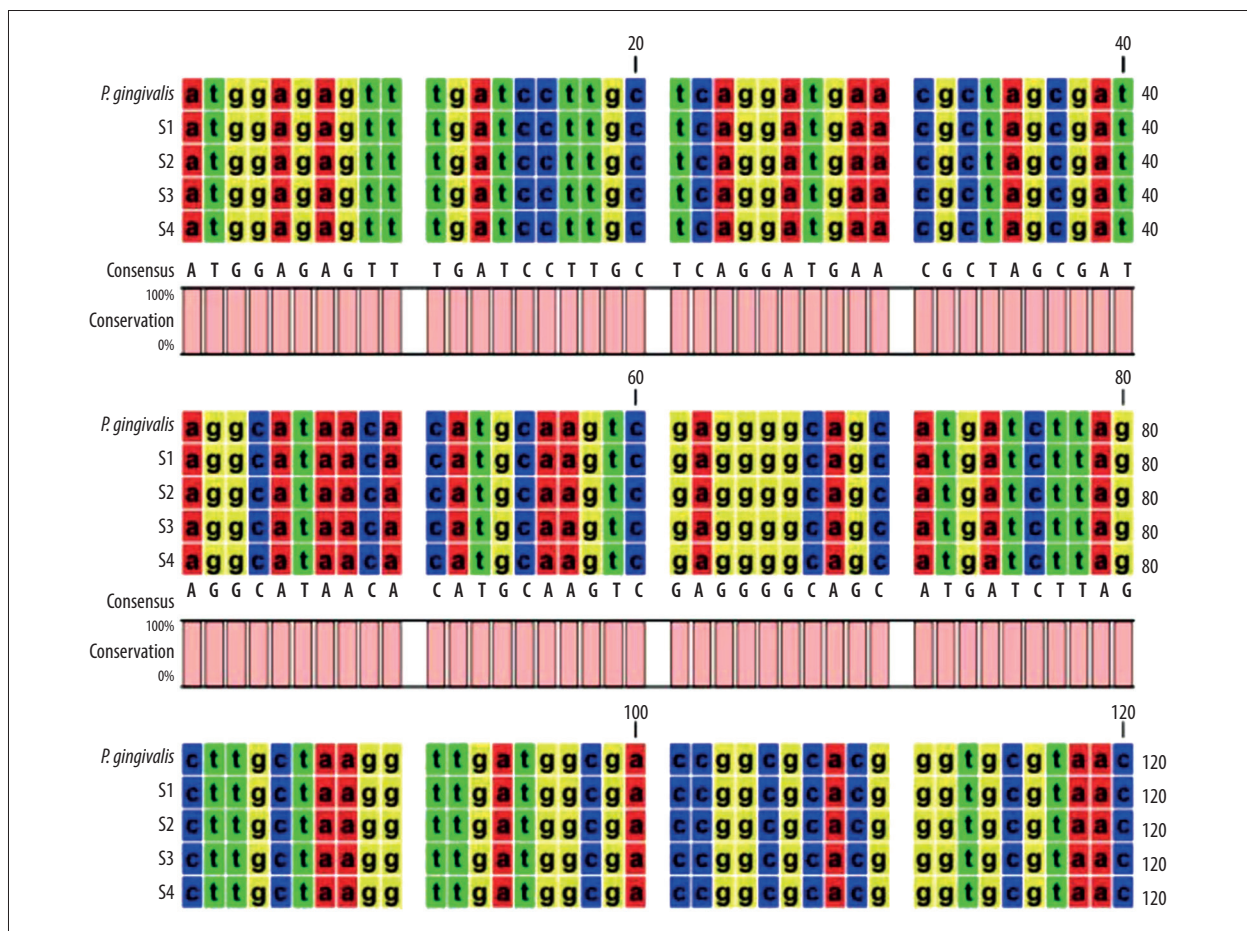
We express our deepest appreciation for Dr. Ying Su (Researcher, PhD), from the College of Software Engineering, Xinjiang University, who provided technical support in data processing.

We also thank the National Natural Science Foundation of China, Tianshan Innovation Team of Xinjiang Uygur Autonomous Region, Shaanxi Clinical Medical Research Center for Dental and Maxillofacial Diseases, and the School/Hospital of Stomatology Fudan University for approving and supporting the study.

**Declaration of Figures' Authenticity**

All figures submitted have been created by the authors, who confirm that the images are original with no duplication and have not been previously published in whole or in part.

**Supplementary Figure**



Supplementary Figure 1. Detection method for *P. gingivalis*.

## References:

1. Meccariello G, Maniaci A, Bianchi G, et al. Neck dissection and trans oral robotic surgery for oropharyngeal squamous cell carcinoma. *Auris Nasus Larynx*. 2022;49(1):117-25
2. Sopka DM, Li T, Lango MN, et al. Dysplasia at the margin? Investigating the case for subsequent therapy in 'low-risk' squamous cell carcinoma of the oral tongue. *Oral Oncol*. 2013;49(11):1083-87
3. Shield KD, Ferlay J, Jemal A, et al. The global incidence of lip, oral cavity, and pharyngeal cancers by subsite in 2012. *Cancer J Clin*. 2017;67(1):51-64
4. Panarese I, Aquino G, Ronchi A, et al. Oral and oropharyngeal squamous cell carcinoma: Prognostic and predictive parameters in the etiopathogenetic route. *Expert Rev Anticancer Ther*. 2019;19(2):105-19
5. Vázquez-Mahía I, Seoane J, Varela-Centelles P, et al. Predictors for tumor recurrence after primary definitive surgery for oral cancer. *J Oral Maxillofac Surg*. 2012;70(7):1724-32
6. Wang W, Han S, Yao Z, et al. A study of epidemiologic and recurrence factors of oral cancer. *J Oral Maxillofac Surg*. 2012;70(9):2205-10
7. Wang B, Zhang S, Yue K, et al. The recurrence and survival of oral squamous cell carcinoma: a report of 275 cases. *Chin J Cancer*. 2013;32(11):614-18
8. Joo YH, Cho JK, Koo BS, et al. Guidelines for the surgical management of oral cancer: Korean Society of Thyroid-Head and Neck Surgery. *Clin Exp Otorhinolaryngol*. 2019;12(2):107-44
9. Lafuente Ibáñez de Mendoza I, Maritxalar Mendia X, García de la Fuente AM, et al. Role of *Porphyromonas gingivalis* in oral squamous cell carcinoma development: A systematic review. *J Periodontol Res*. 2020;55(1):13-22
10. Moergel M, Kämmerer P, Kasaj A, et al. Chronic periodontitis and its possible association with oral squamous cell carcinoma – a retrospective case control study. *Head Face Med*. 2013;9:39
11. Yao QW, Zhou DS, Peng HJ, et al. Association of periodontal disease with oral cancer: A meta-analysis. *Tumour Biol*. 2014;35(7):7073-77
12. Moraes RC, Dias FL, Figueredo CM, et al. Association between chronic periodontitis and oral/oropharyngeal cancer. *Braz Dent J*. 2016;27(3):261-66
13. Michaud DS, Fu Z, Shi J, et al. Periodontal disease, tooth loss, and cancer risk. *Epidemiol Rev*. 2017;39(1):49-58
14. Aas JA, Paster BJ, Stokes LN, et al. Defining the normal bacterial flora of the oral cavity. *J Clin Microbiol*. 2005;43(11):5721-32
15. Bellotti R, Speth C, Adolph TE, et al. Micro- and mycobiota dysbiosis in pancreatic ductal adenocarcinoma development. *Cancers (Basel)*. 2021;13(14):3431
16. Wang KK, He KY, Yang JY, et al. *Lactobacillus* suppresses tumorigenesis of oropharyngeal cancer via enhancing anti-tumor immune response. *Front Cell Dev Biol*. 2022;10:842153
17. Gao JL, Kwan AH, Yammine A, et al. Structural properties of a haemophore facilitate targeted elimination of the pathogen *Porphyromonas gingivalis*. *Nat Commun*. 2018;9(1):4097
18. Liu S, Zhou X, Peng X, et al. *Porphyromonas gingivalis* promotes immunoevasion of oral cancer by protecting cancer from macrophage attack. *J Immunol*. 2020;205(1):282-89
19. Lanzós I, Herrera D, Santos S, et al. Microbiological effects of an antiseptic mouthrinse in irradiated cancer patients. *Med Oral Patol Oral Cir Bucal*. 2011;16(7):e1036-42
20. Singh S, Singh S, Tiwari MB, et al. Microflora analysis in the postchemotherapy patients of oral cancer. *Natl J Maxillofac Surg*. 2019;10(2):141-45
21. Tuominen H, Rautava J. Oral microbiota and cancer development. *Pathobiology*. 2021;88(2):116-26
22. Olsen I, Yilmaz Ö. Possible role of *Porphyromonas gingivalis* in orodigestive cancers. *J Oral Microbiol*. 2019;11(1):1563410
23. Chang C, Geng F, Shi X, et al. The prevalence rate of periodontal pathogens and its association with oral squamous cell carcinoma. *Appl Microbiol Biotechnol*. 2019;103(3):1393-404
24. Hu X, Shen X, Tian J. The effects of periodontitis associated microbiota on the development of oral squamous cell carcinoma. *Biochem Biophys Res Commun*. 2021;576:80-85
25. Wang M, Zhao J, Zhang L, et al. Role of tumor microenvironment in tumorigenesis. *J Cancer*. 2017;8(5):761-73
26. Mughees M, Sengupta A, Khawal S, et al. Mechanism of tumour microenvironment in the progression and development of oral cancer. *Mol Biol Rep*. 2021;48(2):1773-86
27. Noy R, Pollard JW. Tumor-associated macrophages: From mechanisms to therapy. *Immunity*. 2014;41(1):49-61. [Erratum in: *Immunity*. 2014;41(5):866]
28. Wu K, Lin K, Li X, et al. Redefining tumor-associated macrophage subpopulations and functions in the tumor microenvironment. *Front Immunol*. 2020;11:1731
29. Funes SC, Rios M, Escobar-Vera J, et al. Implications of macrophage polarization in autoimmunity. *Immunology*. 2018;154(2):186-95
30. Pan Y, Yu Y, Wang X, et al. Tumor-associated macrophages in tumor immunity. *Front Immunol*. 2020;11:583084. [Erratum in: *Front Immunol*. 2021;12:775758]
31. Guan Y, Li M, Qiu Z, et al. Comprehensive analysis of DOK family genes expression, immune characteristics, and drug sensitivity in human tumors. *J Adv Res*. 2021;36:73-87
32. Mashima R, Hishida Y, Tezuka T, et al. The roles of Dok family adapters in immunoreceptor signaling. *Immunol Rev*. 2009;232(1): 273-85
33. Guittard G, Pontarotti P, Granjeaud S, et al. Evolutionary and expression analyses reveal a pattern of ancient duplications and functional specializations in the diversification of the Downstream of Kinase (DOK) genes. *Dev Comp Immunol*. 2018;84:193-98
34. Lemay S, Davidson D, Latour S, et al. Dok-3, a novel adapter molecule involved in the negative regulation of immunoreceptor signaling. *Mol Cell Biol*. 2000;20(8):2743-54
35. Liu X, Chen F, Li W. Elevated expression of DOK3 indicates high suppressive immune cell infiltration and unfavorable prognosis of gliomas. *Int Immunopharmacol*. 2020;83:106400
36. Loh JT, Teo JKH, Lim HH, et al. Emerging roles of downstream of kinase 3 in cell signaling. *Front Immunol*. 2020;11:566192
37. Cai X, Xing J, Long CL, et al. DOK3 modulates bone remodeling by negatively regulating osteoclastogenesis and positively regulating osteoblastogenesis. *J Bone Miner Res*. 2017;32(11):2207-18
38. Ritchie ME, Phipson B, Wu D, et al. limma powers differential expression analyses for RNA-sequencing and microarray studies. *Nucleic Acids Res*. 2015;43(7):e47
39. Cedoz PL, Prunello M, Brennan K, et al. MethylMix 2.0: An R package for identifying DNA methylation genes. *Bioinformatics*. 2018;34(17):3044-46
40. Wu T, Hu E, Xu S, et al. clusterProfiler 4.0: A universal enrichment tool for interpreting omics data. *Innovation (Camb)*. 2021;2(3):100141
41. Ozhan A, Tombaz M, Konu O. SmultCan: A Shiny application for multi-variable survival analysis of TCGA data with gene sets. *Comput Biol Med*. 2021;137:104793
42. Blanche P, Dartigues JF, Jacqmin-Gadda H. Estimating and comparing time-dependent areas under receiver operating characteristic curves for censored event times with competing risks. *Stat Med*. 2013;32(30):5381-97
43. Langfelder P, Horvath S. WGCNA: An R package for weighted correlation network analysis. *BMC Bioinformatics*. 2008;9:559
44. Mayakonda A, Lin DC, Assenov Y, et al. Maftools: Efficient and comprehensive analysis of somatic variants in cancer. *Genome Res*. 2018;28(11):1747-56
45. Sahingur SE, Yeudall WA. Chemokine function in periodontal disease and oral cavity cancer. *Front Immunol*. 2015;6:214
46. Hayes RB, Ahn J, Fan X, et al. Association of oral microbiome with risk for incident head and neck squamous cell cancer. *JAMA Oncol*. 2018;4(3):358-65
47. Singh R, Mishra MK, Aggarwal H. Inflammation, immunity, and cancer. *Mediators Inflamm*. 2017;2017:6027305
48. Johnson DE, Burtneis B, Leemans CR, et al. Head and neck squamous cell carcinoma. *Nat Rev Dis Primers*. 2020;6(1):92
49. Shao W, Fujiwara N, Mouri Y, et al. Conversion from epithelial to partial-EMT phenotype by *Fusobacterium nucleatum* infection promotes invasion of oral cancer cells. *Sci Rep*. 2021;11(1):14943
50. Chattopadhyay I, Verma M, Panda M. Role of oral microbiome signatures in diagnosis and prognosis of oral cancer. *Technol Cancer Res Treat*. 2019;18:1533033819867354
51. Wen L, Mu W, Lu H, et al. *Porphyromonas gingivalis* promotes oral squamous cell carcinoma progression in an immune microenvironment. *J Dent Res*. 2020;99(6):666-75

52. Liu D, Liu S, Liu J, et al. sRNA23392 packaged by *Porphyromonas gingivalis* outer membrane vesicles promotes oral squamous cell carcinomas migration and invasion by targeting desmocollin-2. *Mol Oral Microbiol.* 2021;36(3):182-91
53. Bugueno IM, Batool F, Keller L, et al. *Porphyromonas gingivalis* bypasses epithelial barrier and modulates fibroblastic inflammatory response in an in vitro 3D spheroid model. *Sci Rep.* 2018;8(1):14914
54. Wang H, Zhou H, Duan X, et al. *Porphyromonas gingivalis*-induced reactive oxygen species activate JAK2 and regulate production of inflammatory cytokines through c-Jun. *Infect Immun.* 2014;82(10):4118-26
55. Li Y, Mooney EC, Xia XJ, et al. A20 Restricts inflammatory response and desensitizes gingival keratinocytes to apoptosis. *Front Immunol.* 2020;11:365
56. Konishi H, Urabe S, Teraoka Y, et al. *Porphyromonas gingivalis*, a cause of preterm birth in mice, induces an inflammatory response in human amnion mesenchymal cells but not epithelial cells. *Placenta.* 2020;99:21-26
57. Coussens LM, Werb Z. Inflammation and cancer. *Nature.* 2002;420(6917):860-67
58. Landskron G, De la Fuente M, Thuwajit P, et al. Chronic inflammation and cytokines in the tumor microenvironment. *J Immunol Res.* 2014;2014:149185
59. Guo ZC, Jumatai S, Jing SL, et al. Bioinformatics and immunohistochemistry analyses of expression levels and clinical significance of CXCL2 and TANs in an oral squamous cell carcinoma tumor microenvironment of *Porphyromonas gingivalis* infection. *Oncol Lett.* 2021;21(3):189
60. Castro SA, Collighan R, Lambert PA, et al. *Porphyromonas gingivalis* gingipains cause defective macrophage migration towards apoptotic cells and inhibit phagocytosis of primary apoptotic neutrophils. *Cell Death Dis.* 2017;8(3):e2644
61. Vitale I, Manic G, Coussens LM, et al. Macrophages and metabolism in the tumor microenvironment. *Cell Metab.* 2019;30(1):36-50
62. Núñez-Acurio D, Bravo D, Aguayo F. Epstein-Barr virus-oral bacterial link in the development of oral squamous cell carcinoma. *Pathogens.* 2020;9(12):1059
63. Palomero T, Couronné L, Khiabani H, et al. Recurrent mutations in epigenetic regulators, RHOA and FYN kinase in peripheral T cell lymphomas. *Nat Genet.* 2014;46(2):166-70
64. Sumiyoshi H, Matsushita A, Nakamura Y, et al. Suppression of STAT5b in pancreatic cancer cells leads to attenuated gemcitabine chemoresistance, adhesion and invasion. *Oncol Rep.* 2016;35(6):3216-26
65. Zhou M, Liu X, Li Z, et al. Caspase-3 regulates the migration, invasion and metastasis of colon cancer cells. *Int J Cancer.* 2018;143(4):921-30
66. Kang BW, Jeon HS, Chae YS, et al. Impact of genetic variation in microRNA-binding site on susceptibility to colorectal cancer. *Anticancer Res.* 2016;36(7):3353-61
67. Gao WS, Qu YJ, Huai J, et al. DOK3 is involved in microglial cell activation in neuropathic pain by interacting with GPR84. *Aging (Albany NY).* 2020;13(1):389-410
68. Vidyarthi A, Agnihotri T, Khan N, et al. Predominance of M2 macrophages in gliomas leads to the suppression of local and systemic immunity. *Cancer Immunol Immunother.* 2019;68(12):1995-2004